

# Journal Pre-proof

Selenium nanoparticles induced variations in growth, morphology, anatomy, biochemistry, gene expression, and epigenetic DNA methylation in *Capsicum annuum*; an in vitro study

Soheila Sotoodehnia-Korani, Alireza Iranbakhsh, Mostafa Ebadi, Ahmad Majd, Zahra Oraghi Ardebili



PII: S0269-7491(20)31516-5

DOI: <https://doi.org/10.1016/j.envpol.2020.114727>

Reference: ENPO 114727

To appear in: *Environmental Pollution*

Received Date: 29 February 2020

Revised Date: 1 May 2020

Accepted Date: 1 May 2020

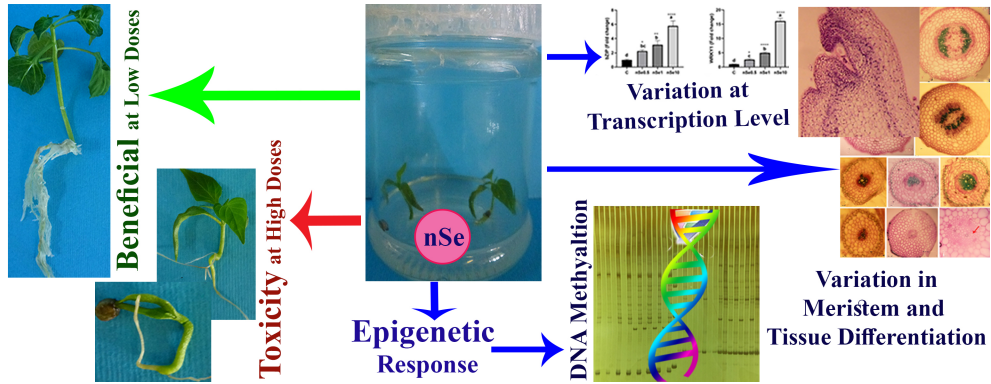
Please cite this article as: Sotoodehnia-Korani, S., Iranbakhsh, A., Ebadi, M., Majd, A., Ardebili, Z.O., Selenium nanoparticles induced variations in growth, morphology, anatomy, biochemistry, gene expression, and epigenetic DNA methylation in *Capsicum annuum*; an in vitro study, *Environmental Pollution* (2020), doi: <https://doi.org/10.1016/j.envpol.2020.114727>.

This is a PDF file of an article that has undergone enhancements after acceptance, such as the addition of a cover page and metadata, and formatting for readability, but it is not yet the definitive version of record. This version will undergo additional copyediting, typesetting and review before it is published in its final form, but we are providing this version to give early visibility of the article. Please note that, during the production process, errors may be discovered which could affect the content, and all legal disclaimers that apply to the journal pertain.

© 2020 Published by Elsevier Ltd.

**CRediT authorship contribution statement**

**Soheila Sotoodehnia Korani:** Resources, methodology, review, and editing; **Alireza Iranbakhsh:** Conceptualization, visualization, investigation, formal analysis, writing- original draft, review, and editing; **Mostafa Ebadi:** Conceptualization, visualization, investigation, software analysis, review, and editing; **Ahmad Majd:** Conceptualization, Investigation, review & editing. **Zahra Oraghi Ardebili:** Conceptualization, visualization, investigation, formal analysis, writing, review, and editing.



1   **Selenium nanoparticles induced variations in growth, morphology, anatomy, biochemistry,**  
2   **gene expression, and epigenetic DNA methylation in *Capsicum annuum*; an in vitro study**

3   **Soheila Sotoodehnia-Korani<sup>1</sup>, Alireza Iranbakhsh<sup>1\*</sup>, Mostafa Ebadi<sup>2</sup>, Ahmad Majd<sup>3</sup>, Zahra**  
4   **Oraghi Ardebili<sup>4</sup>**

5   <sup>1</sup>Department of Biology, Science and Research Branch, Islamic Azad University, Tehran, Iran.

6   <sup>2</sup>Department of Biology, Damghan Branch, Islamic Azad University, Damghan, Iran.

7   <sup>3</sup>Department of Biology, North Tehran Branch, Islamic Azad University, Tehran, Iran.

8   <sup>4</sup>Department of Biology, Garmsar Branch, Islamic Azad University, Garmsar, Iran.

9   \*Corresponding author: [iranbakhsh@iau.ac.ir](mailto:iranbakhsh@iau.ac.ir); +989127961108; Postal code: 1477893855

10

## 11   **Abstract**

12   This study aimed to explore whether supplementation of the culture medium with selenium  
13   nanoparticles (nSe) can influence growth, biochemistry, expression of transcription factors, and  
14   epigenetic DNA methylation in *Capsicum annuum*. The seeds were grown in hormone-free MS  
15   culture medium supplemented with nSe (0, 0.5, 1, 10, and 30 mgL<sup>-1</sup>) or corresponding doses of  
16   bulk type selenate (BSe). Incorporation of nSe into the medium caused variations in morphology  
17   and growth in a manner dependent on the dose and Se type. The low doses of nSe displayed  
18   growth-promoting effects, whereas nSe at 10 and 30 mgL<sup>-1</sup> were associated with severe toxicity  
19   and abnormality in leaf and root development. MSAP analysis confirmed the substantial  
20   variation in cytosine DNA methylation in response to the toxic dose of nSe exhibiting epigenetic  
21   modification. The nSe toxicity was associated with DNA hyper-methylations. The nSe

22 treatments transcriptionally upregulated the bZIP1 transcription factor by an average of 3.5 folds.  
23 With a similar trend, the upregulation (mean = 9.8 folds) in the expression of the WRKY1  
24 transcription factor resulted from the nSe application. The nSe0.5 or nSel treatments resulted in  
25 a significant induction (mean = 48%) in nitrate reductase activity. A high dose of nSe led to an  
26 increase in proline concentration. The nSe treatments were also associated with modifications in  
27 activities of peroxidase and catalase enzymes. Besides, the nSe utilization increased the activity  
28 of phenylalanine ammonia-lyase enzyme (mean = 76%) and concentrations of soluble phenols  
29 (mean = 51%). The toxic dose of nSe also caused abnormalities in the structure of the stem  
30 apical meristem. The nSe toxicity was also associated with inhibition in the differentiation of  
31 xylem tissues. These findings provide novel insights into the nSe-associated molecular variations  
32 in conferring the modified growth, anatomy, and metabolism.

33 **Summary**

34 This is the first report on the nSe-associated changes in toxicity, epigenetic DNA hyper-  
35 methylation, transcriptional regulation of transcription factors, biochemistry, and anatomy.

36 **Keywords**

37 DNA methylation; Epigenetic; Selenium nanoparticle; Transcription factors; Toxicity

38 **1. Introduction**

39 The need for selenium (Se) has been proven for many living organisms, including humans, but  
40 its role in the life cycle of plants is still controversial (Kolbert et al., 2018; Babajani et al.,  
41 2019b). Taking agriculture into account, several lines of evidence highlighted the potential of Se  
42 serving as a novel fertilizer to improve plant productivity and protection as well as produce Se-  
43 biofortified crops (Djanaguiraman et al., 2018; Kolbert et al., 2018; Nazerieh et al., 2018;

44 Babajani et al., 2019a,b). Among the different mineral forms of Se, selenate and selenite are the  
45 most common types used in scientific research (Cao et al., 2018). However, the optimal  
46 concentration of Se is largely varied depending on several determining factors, including plant  
47 species, developmental stage, application procedure, and other environmental factors (Safari et  
48 al., 2018). Recent reports highlighted the notion that, owing to their unique properties, nano-  
49 products may exclusively induce distinct responses in cells from their bulk counterparts  
50 (Babajani et al., 2019a; Ghasempour et al., 2019; Moghanloo et al., 2019a,b; Seddighinia et al.,  
51 2020). The elemental red Se nano-product (nSe) has been widely exploited in medicinal-related  
52 industries because of exhibiting high bioactivity, great antioxidant activity, anti-cancer role, and  
53 antimicrobial traits (Hu et al. 2018). Recently, several reports underline the beneficial effects of  
54 nSe on modifying expression of genes (Safari et al., 2018; Babajani et al., 2019a), antioxidant  
55 machinery (Djanaguiraman et al., 2018; Babajani et al., 2019a), primary metabolism (Nazerieh et  
56 al., 2018; Babajani et al., 2019a), and secondary metabolism (Babajani et al., 2019a). Taking  
57 current knowledge gaps into account, convincing scientific experiments are needed to elucidate  
58 the possible interactions among plant cells, nSe, and its bulk form. Moreover, potential plant  
59 responses to nSe incorporation into the culture medium remain elusive and need more in-depth  
60 investigation.

61 A multitude of transcription factors contribute to transcriptional switches in stress/stimuli-  
62 responsive genes by which plants can acclimate to different environmental cues. Therefore,  
63 functional monitoring of interplay among transcription factors during differential conditions is of  
64 critical importance to identify the exact molecular mechanisms involved in stimuli-activated  
65 signaling cascades (Iranbakhsh et al., 2020). The signal perception and transduction are  
66 performed through the involvement of diverse G-protein coupled receptors, ligand-gated

67 channels, kinases, secondary messengers, hormones, and transcription factors (Khan et al.,  
68 2018). These events are followed by triggering of the stress/elicitor/stimuli-signaling pathways.

69 In the present study, we aimed to explore potential nSe-mediated changes in expression of two  
70 key transcription factors, WRKY1 and bZIP, as target. In higher plants, WRKY transcription  
71 factors encoded by the WRKY gene superfamily contribute efficiently to modulations of  
72 responsive genes to stress, stimuli, and/or developmental transition cues via binding to cis-  
73 elements in the promoter region (Kumar et al., 2019; Song et al., 2018). The transcription factor  
74 family of bZIP (basic leucine zipper) is distinguished by the basic DNA-binding region (sixteen  
75 basic amino acids) and leucine zipper (a dimerization domain). These transcription factors play  
76 vital roles in a wide range of biological reactions, including cellular elongation, senescence,  
77 tissue differentiation, organ development, flowering, seed maturation, and response to  
78 environmental cues (Khan et al., 2018).

79 An orchestrated complex system epigenetically modulates the topological properties of  
80 chromatin. DNA methylation/demethylation at CG sites are vital processes contributing to  
81 chromatin remodeling by which transcriptions of genes are controlled. It is therefore important to  
82 understand how nSe might epigenetically influence plants. However, there are only limited  
83 studies on how exposure to nSe may be connected to changes in cellular transcription. Hereby,  
84 we aimed to evaluate possible variations in DNA methylation of CG sites in response to long-  
85 term exposure to nSe.

86 Pepper (*Capsicum annuum*) is a significant cultivating crop widely exploited in food and  
87 pharmaceutical industries due to its specific phytochemistry, in particular, active alkaloid  
88 component of capsaicin (8-methyl-N-vanillyl-6-nonenamide) (Safari et al., 2017; Iranbakhsh et  
89 al., 2018). Its bioactive alkaloids exert great anti-inflammatory, anticancer, antioxidant, and

90 antimicrobial effects (Safari et al., 2017). It also possesses the superb potential of protecting and  
91 influencing human body systems, such as the cardiovascular, gastrointestinal, and the nervous  
92 systems (Safari et al., 2017).

93 Within this framework, the present study aims to explore whether supplementation of the culture  
94 medium with nSe can influence seedling morphology, growth, stem apical meristem,  
95 biochemistry, expression of two key transcription factors, and epigenetic cytosine DNA  
96 methylation in *C. annuum*.

## 97 **2. Material and methods**

### 98 **2.1. Materials, experimental conditions, and treatments**

99 The nano-product (nSe; APS:10–45nm; true density:  $3.89 \text{ gcm}^{-3}$ ; morphology: near spherical;  
100 CAS#7446-08-4) was purchased in form of stock red solution ( $1000 \text{ mgL}^{-1}$  containing 0.1%  
101 polyvinylpyrrolidone (PVP) as stabilizer) from the reliable company (NanoSany Corporation,  
102 Iranian Nanomaterials Pioneers Company, Mashhad City, Khorasan Province, Iran). Besides,  
103 the scan spectrum curve (UV-Vis spectrophotometry), zeta potential index (Zetasizer; Malvern,  
104 UK), and electron microscopy were also provided.

105 The pepper seeds (*C. annuum* PP805 Godiva; Pop Vriend Seeds, Netherlands) were disinfected  
106 through several consecutive steps using different compounds, including water containing liquid  
107 detergent (for 4 min), sodium hypochlorite (0.6%; 15 min), ethanol (70% for 1 min). After each  
108 disinfection step, the seeds were rinsed with sterile distilled water. The disinfected seeds were  
109 grown in hormone-free MS culture medium (Murashig and Skoog, 1962) supplemented with  
110 different concentrations of nSe (0, 0.5, 1, 10, and  $30 \text{ mgL}^{-1}$ ) or corresponding doses of selenate  
111 as a bulk type (BSe) under a sterile condition. It should be noted that to address both the  
112 potential benefits and toxicity in a dose dependent manner, nSe doses were selected according to

113 the pre-test experiment at different concentrations ranging from 0.1 to 50 mgL<sup>-1</sup>. Treatments  
 114 groups were as follows:

115 C- Control; BSe0.5- BSe at 0.5 mgL<sup>-1</sup>; nSe0.5- nSe at 0.5 mgL<sup>-1</sup>; BSe1- BSe at 1 mgL<sup>-1</sup>; nSe1-  
 116 nSe at 1 mgL<sup>-1</sup>; BSe10- BSe at 10 mgL<sup>-1</sup>; nSe10- nSe at 10 mgL<sup>-1</sup>; BSe30- BSe at 30 mgL<sup>-1</sup>;  
 117 nSe30- nSe at 30 mgL<sup>-1</sup>

118 The BSe/nSe-treated seedlings were kept in a controlled condition of growth chamber. The 35-  
 119 day-old seedlings were harvested and subjected for the further analysis. It should be noted that  
 120 biochemical, anatomical, and molecular analyses were only performed in the nSe-treated  
 121 seedlings.

122 **2.2. DNA methylation**

123 The patterns of DNA cytosine methylation were estimated based on the Methylation-Sensitive  
 124 Amplification Polymorphism (MSAP) method and digestions by isoschizomers of *Hpa*II and  
 125 *Msp*I (having differential methylation sensitivity) (Guevara et al., 2017). In this experiment,  
 126 DNA methylation patterns of control and nSe10 (exhibited moderate toxicity) were compared.  
 127 DNA was extracted from the well-grounded leaves in liquid nitrogen using kit (GeneAll, South  
 128 Korea). MSAP analysis in each treatment group was carried out on samples digested in  
 129 *Eco*RI/*Hpa*II and *Eco*RI/*Msp*I conditions. In MSAP technique, there are several steps, including  
 130 digestion with isoshimerases, adapter ligations, pre-amplification, selective amplification,  
 131 fragment visualization, scoring, and data mining. 500 ng of the extracted DNA were digested by  
 132 the restriction enzymes in the presence of *Eco*RI/*Hpa*II or *Eco*RI/*Msp*I (37 °C for 2h). After that,  
 133 5 µl of digested genomic DNA were ligated to adapters (MsHPI: 5'-3' sequences of  
 134 GACGATGAGTCTAGAA; MsHPII: CGTTCTAGACTCATC; EcoRI-A1:  
 135 CTCGTAGACTGCGTACC; EcoRI-A2: AATTGGTACGCAGTCTAC) by T4 ligase

136 (Fermentase, USA) and incubation at 22 °C for 1 h followed by incubation at 4 °C overnight. At  
 137 pre-amplification stage, samples were amplified using thermocycler (PeQlab; Germany) with  
 138 primers (5'-3' sequences MsHp pre: GATGAGTCTAGAACGGT; EcoR1 pre:  
 139 GACTGCGTACCAATTCA) under particular program (95 °C for 5 min; 35 cycles of 94 °C for  
 140 20 s, 58 °C for 40 s, 72 °C for 2 min, and finally 72 °C for 10 min). To verify the efficiency of  
 141 amplification, electrophoresis on 1% agarose gel was conducted. At selective amplification  
 142 stage, amplifications were performed using PCR and applications of specific primers  
 143 (EcoR1ACT: GACTGCGTACCAATTCACT; EcoR1AAG: GACTGCGTACCAATTCAAG;  
 144 MsHp-TAC: GATGAGTCTAGAACGGTAC: MsHp-TC: GATGAGTCTAGAACGGTC) with  
 145 a similar program at pre-amplification stage. This stage was followed by electrophoresis. The  
 146 amplified fragments were separated, visualized (silver staining), and scored. Finally, data was  
 147 interpreted and the principal coordinate analysis (PCoA), dendrogram, and percentage of  
 148 molecular variance were designed using R, DARwin, and GenAlEx software.

### 149        2.3. Transcriptions of target genes

150 Transcriptions of the target genes were monitored in leaves (stored in -80 °C prior to RNA  
 151 extraction). RNA extractions and purifications from liquid nitrogen-grounded samples were  
 152 performed using Trizol (GeneAll Biotechonlogy Co, South Korea), DEPC Water (Bio Basic,  
 153 Canada), and Dnase I (Fermentase, USA). After that, the RNA purity was assessed based on  
 154 absorbance ratio (260/280 nm) with Nanodrop (Thermo Scientific™NanoDrop Model 2000c).  
 155 Next, the synthesis of complementary DNA (cDNA) was performed with thermocycler  
 156 (PEQLAB, 96Grad). The primers of the target genes were designed using Oligo7 and AllelID  
 157 software. The forward and reverse sequences of primers for WRKY1 (transcription factor  
 158 CaWRKY1; AY229992) were GCCGAGATTGCATTCATGACA and

159 GGTCACTGAAGCATCGCTCT, respectively. The forward and reverse sequences for bZIP  
 160 (bZIP transcription factor (ATBZ1); MK248905) were GGAAGCTGAAGTGGCAAAGC and  
 161 CCAAGGTCCAGTCACTGTCC, respectively. Besides, GCTAACAACTTGCCCCGTGGAC  
 162 and CCAGCAGAAGAGATCCAAGACC were the forward and reverse sequences of Tubulin (a  
 163 housekeeping gene), respectively. The expression rates of the mentioned target genes were  
 164 quantified based on SYBR green (GeneAll, South Korea) and the real-time quantitative PCR  
 165 procedure (Applied Biosystems StepOne<sup>TM</sup> Real-Time PCR). After that according to the CT  
 166 method, the variations in expression level of the target genes were expressed as fold differences.

#### 167       **2.4. preparation of enzyme extracts and activities of several key enzymes**

168 Enzymes were purified from the well-powdered leaves and roots in liquid nitrogen using the  
 169 extraction phosphate buffer (100 mM; pH of 7.5) containing ascorbate and Na<sub>2</sub>EDTA. Then, the  
 170 homogenate was subjected for centrifugation at 4 °C and the supernatants kept at–80 °C until  
 171 enzyme analysis. The nitrate reductase activity in leaves was quantified according to the  
 172 procedure of Sym (1984) and expressed in micro mole nitrite per hour per gram fresh mass  
 173 ( $\mu\text{mol NO}_2^- \text{h}^{-1} \text{g}^{-1} \text{fw}$ ). Peroxidase activity (Babajani et al., 2019a) and catalase activity (Salah et  
 174 al., 2015) were also determined in roots and expressed in Unit E  $\text{g}^{-1} \text{fw}$ . Furthermore,  
 175 phenylalanine ammonia lyase (PAL) activity was in leaves assessed based on the procedure  
 176 explained by Beaudoin-Eagan and Thorpe (1985) and expressed in microgram cinnamate per  
 177 min per gram fresh weight ( $\mu\text{g Cin} \cdot \text{min}^{-1} \text{g}^{-1} \text{fw}$ ).

#### 178       **2.5. Quantifications of proline and soluble phenols**

179 Purification and determination of leaf proline accumulation in the nSe-treated seedlings were  
 180 spectrophotometrically evaluated according to the protocol explained by Bates et al., (1973). The  
 181 absorbance amounts at 520 nm refer to the proline content. The proline concentration was

182 calculated based on the standard curve. Ethanol (80% v/v) was utilized as a solvent to extract the  
183 total soluble phenolic compounds from leaves. Total soluble phenols were measured using  
184 Folin-Ciocalteu reagent and the standard curve of tannic acid as a standard material (Nazerieh et  
185 al., 2018).

186 **2.6. Histological study**

187 The stem apical meristem was fixed in FAA fixator. Then, the samples were prepared for  
188 sectioning by several successive stages (dehydration, infiltration, and embedding). After that,  
189 cross sections of samples were carried out using a microtome instrument. The microtome-made  
190 cross sections were subjected for staining using Hematoxylin and Eosin protocol, observed  
191 using a light microscope, and finally photographed. In addition, the cross sections of the basal  
192 stem (1 cm above transition zone root/shoot) and root were prepared to evaluate the nSe-  
193 associated changes in tissue differentiation. The cross sections were sequentially stained with  
194 different compounds, including sodium hypochlorite (15 min), acetic acid (5 min), carmine (15  
195 min), and methylene blue (30 s). Finally, the stained sections were monitored by a light  
196 microscope and photographed.

197 **2.7. Statistical analysis**

198 The experimental design was completely randomized. All data were subjected to analysis of  
199 variance (ANOVA) using SPSS and GraphPad software. The mean values of three independent  
200 replications for each treatment group were submitted to variance analysis by the Tukey test at a  
201 level of 5% of probability.

202 **3. Results**

203 **3.1. Physicochemical characteristics of the nano-product**

204 In Fig. 1, the physicochemical properties of nSe are shown. According to the scan spectrum  
 205 curves of nSe at two doses ( $10$  and  $20\text{ mgL}^{-1}$ ), a sharp absorption peak was recorded in the UV  
 206 range around  $200$ - $300\text{ nm}$  manifesting nano nature (Fig. 1A). Taking stability of nSe solution  
 207 into account, no deposition was observed in the nano solution, and no change in the absorption  
 208 spectrum was recorded over several hours, confirming the stability of the nano-compound.  
 209 Moreover, the magnitude of the zeta potential index (the negative surface charge) also confirmed  
 210 the colloidal stability of the nano-product through electrostatic repulsion (Fig. 1B). The nearly  
 211 spherical morphology of nSe with an approximate size of  $20\text{ nm}$  is presented in Fig. 1C.

### 212     **3.2. Morphology and Growth**

213 Incorporation of nSe into the rooting culture medium caused differential morphology and growth  
 214 in a concentration-dependent manner (Fig. 2). Common visible toxicity symptoms, including  
 215 necrosis and chlorosis, were not observed. The nSe at  $0.5$  and  $1\text{ mgL}^{-1}$  displayed growth-  
 216 promoting effects, while nSe treatment at  $10$  and  $30\text{ mgL}^{-1}$  resulted in severe toxicity and  
 217 abnormality in leaf and root development (Fig. 2). In the nSe0.5 and nSe1 treatment groups the  
 218 total leaf fresh mass was increased by an average of  $65.5\%$  when compared to the control (Fig.  
 219 2). However, bulk counterpart (BSe) at  $0.5\text{ mgL}^{-1}$  enhanced total leaf fresh mass by  $19\%$ . While  
 220 the BSe1 treatment reduced total leaf fresh mass by an average of  $27.8\%$ . With increasing  
 221 concentrations of nSe from  $0.5$  to  $1\text{ mgL}^{-1}$ , the root fresh mass was significantly increased  
 222 relative to the control (Fig. 2). Except for BSe0.5, the other concentrations of BSe adversely  
 223 influenced the root fresh mass (Fig. 2).

### 224     **3.3. MSAP-based DNA methylation**

225 Variations in DNA methylation between the nSe ( $10\text{ mgL}^{-1}$ ) and control was compared based on  
 226 the MSAP method with application of Eco RI/ Hpa II and Eco RI/ Msp I. According to the

227 MSAP assessment, the number of Methylation-Susceptible Loci (MSL) were 53 whereas the  
 228 number of Non-Methylated Loci (NML) was zero. Number of polymorphic MSL was 4 which is  
 229 equal to 8% of total MSL. Under Eco RI/Hpa II conditions, the principal coordinates analysis  
 230 (PCoA) plots (Fig. 3A) and dendrogram (Fig. 3B) displayed differential patterns of DNA  
 231 methylation. In this regard, percentage of molecular variance within and among treatment groups  
 232 were estimated to be 49% and 51%, respectively (Fig. 3C). As it can be noticed in Fig. 4A and  
 233 4B, nSe supplementation was associated with variations in DNA methylation profile under *Eco*  
 234 *RI/Msp* I conditions. Under *EcoRI/MspI* conditions, the percentage of molecular variance within  
 235 and among groups were 32% and 68%, respectively (Fig. 4C). The PCoA plots confirmed the  
 236 epigenetic variations in DNA methylation within the leaves of seedlings grown in the culture  
 237 medium containing toxic dose of nSe (nSe10) in comparison to the untreated control (Fig. 5A, B,  
 238 C). The data demonstrated the nSe-associated epigenetic modification in pepper seedlings grown  
 239 under *in vitro* conditions.

#### 240       **3.4. Expression of Transcription Factors (*WRKY1* and *bZIP1*)**

241 The nSe0.5, nSe1, and nSe10 treatments upregulated the expression of the *bZIP1* gene in  
 242 comparison to the control by 2.2, 3.0, and 5.4 folds, respectively (Fig. 6A). Slight upregulation  
 243 (mean = 3.8-fold) in the expression of *WRKY1* was observed after the nSe0.5 and nSe1  
 244 treatments (Fig. 6B). However, exposure to nSe10 led to drastic induction of the *WRKY1* gene by  
 245 15.8 folds relative to the control (Fig. 6B). The nSe0.5 or nSe1 treatments resulted in a  
 246 significant induction (mean = 48%) in the nitrate reductase activity. However, nSe of 10 mgL<sup>-1</sup>  
 247 declined the nitrate reductase activity by 26.2% in comparison to the control (Fig. 6C). A  
 248 significant increase in proline concentration was observed in response to the nSe10 treatment  
 249 (Fig. 6D), Although the other nSe treatments were not associated with a statistically significant

250 difference in the proline content (Fig. 6D). The nSe0.5 or nSe1 groups exhibited slightly higher  
 251 (mean = 21%) peroxidase activities than the control (Fig. 6E). In contrast, the nSe10 treatment  
 252 slightly declined the peroxidase activity by 24.7% relative to the control (Fig. 6E). The nSe1  
 253 (56%) and nSe10 (2.4 folds) induced catalase activities (Fig. 6F). With a linear trend, the activity  
 254 of the PAL enzyme is enhanced with increasing concentrations of nSe (Fig. 6G). Plants treated  
 255 with nSe had higher concentrations of soluble phenolic compounds (mean = 51%) than the  
 256 control (Fig. 6H).

### 257       **3.5. Stem apical meristem (SAM) and anatomical changes in stem and root**

258 The longitudinal section of the stem apical meristem showed that both the meristem structure and  
 259 morphology were affected by the nSe treatments. Besides, nSe at 10 mgL<sup>-1</sup> caused abnormalities  
 260 in the formation of leaf primordia through the action of stem apical meristem (Fig. 7C). Taking  
 261 anatomical changes of basal stem into account, the nSe treatments led to variations in cell size  
 262 and tissue differentiation in a concentration-dependent manner, especially in conducting tissues  
 263 (Fig. 8A-D). The nSe toxicity was associated with inhibition of xylem differentiation in stem  
 264 (Fig. 8D). Likewise, the nSe treatments in a manner dependent on the doses were associated with  
 265 anatomical alterations in roots (Fig. 8E-I). The nSe application at 1 mgL<sup>-1</sup> developed  
 266 secondary tissues and fibers (Fig. 8G). However, nSe restricted the differentiation of vascular  
 267 conducting tissues at 10 mgL<sup>-1</sup> (Fig. 8 H). Interestingly, the differentiation of xylem tissues was  
 268 completely repressed by nSe at 30 mgL<sup>-1</sup> (Fig. 8 I1, I2).

### 269       **4. Discussion**

270 The high doses of nSe displayed severe toxicity and caused abnormal morphology. Moreover,  
 271 the toxic concentration of nSe impaired the structure of the stem apical meristem organization.  
 272 The high concentrations of nSe appear to restrict organ development through the disruption of

273 apical meristem. Therefore, it seems that the presence of nSe in the culture medium halts or  
274 slows down the plant's growth program by influencing the meristem zone. In *Melissa officinalis*,  
275 nSe application altered apical dominancy indirectly exhibiting changes in phytohormones and  
276 meristem activity (Babajani et al., 2019a). Furthermore, our results show that the response to nSe  
277 is different from that of the corresponding bulk type. The differential plant reaction to BSe and  
278 nSe may be partly attributed to their different uptake kinetics, differential physicochemical traits,  
279 and different interactions with biomolecules. In this regard, the influx mechanism of BSe (active  
280 transport via sulfate/phosphate transporters) is different from the nSe (passive diffusion through  
281 aquaporin membrane channels) (Hu et al., 2018). In wheat, the influx rate of nSe was much  
282 lower than that of the bulk counterpart, selenite (Hu et al., 2018). Moreover, nSe entry into the  
283 cell is associated with its rapid metabolism and production of selenomethionine in *Triticum*  
284 *aestivum* when compared to the bulk form (Hu et al., 2018). As mentioned above, the high  
285 concentrations of nSe impaired the structure and function of stem apical meristem resulting in an  
286 abnormal architecture. Several lines of evidence support Se-associated changes in signaling  
287 hormones, like ethylene, auxin, salicylic acid, and cytokinin (Nazerieh et al., 2018; Babajani et  
288 al., 2019a,b; Feigl et al., 2019; Lehotai et al., 2016; Malheiros et al., 2019; Zahedi et al., 2019;  
289 Soleymanzadeh et al., 2020) which may be responsible for differential growth, metabolism,  
290 tissue differentiation, and morphology.

291 Moreover, nSe treatment was found to be associated with variation in DNA methylation patterns  
292 according to the MSAP-based analysis demonstrating nSe-associated epigenetic differentiation.  
293 Cytosine DNA methylation influences chromatin conformation through which gene accessibility  
294 to the nuclear transcriptional system is determined. According to our results, the nSe toxicity was  
295 associated with hyper-methylations. In line with our results, the cyto-genotoxic effect of multi-

296 walled carbon nanotube in *Allium cepa* was reported to be associated with DNA  
297 hypermethylation (Ghosh et al., 2015). Based on our knowledge, this is the first report on nSe-  
298 associated changes in DNA methylation. Moreover, Ag nanoparticles induced the expression of  
299 six miRNAs as one of the most important epigenetic mechanisms (Brzóska et al., 2019). Hereby,  
300 the findings of the present study underline the necessity of including epigenetic monitoring in  
301 toxicological evaluation of the nanomaterials and various biological systems.

302 The nSe treatments up-regulated the expressions of both *WRKY1* and *bZIP1* transcription factors.  
303 Both *WRKY1* (Iranbakhsh et al., 2020) and *bZIP1* (Sharma et al., 2011) are major components  
304 of signal transduction and subsequent improvements in plant protection against stress conditions.  
305 The *WRKY1* transcription factor is involved in signal transduction of salicylic acid (Bakshi and  
306 Oelmüller, 2014) and jasmonic acid (Marchive et al., 2013), thereby regulating a wide range of  
307 downstream genes (Iranbakhsh et al., 2020). Throughout the plant life cycle, the transcription  
308 factors of *bZIPs* participate in a multitude of biological processes, including senescence, tissue  
309 differentiation, flower development, root initiation, and reactions to physicochemical stress  
310 (Khan et al., 2018). In line with these results, exposure to nSe has been reported to trigger the  
311 expression of the transcription factor of heat shock factor A4A in wheat (Safari et al., 2018).  
312 Moreover, the induced expressions of rosmarinic acid synthase (RAS) and Hydroxy  
313 phenylpyruvate reductase (HPPR) genes have been recorded following the exposure to the nSe  
314 application in *Melissa officinalis* (Babajani et al., 2019a).

315 It seems that the nSe-mediated alterations of the cellular redox status and phytohormones trigger  
316 particular signaling by which the nuclear transcription program may be remodeled. Several  
317 previous reports underline Se-associated changes in phytohormones, NO, and transcriptions of

318 genes in different plant species (Lehotai et al., 2012; Nazerieh et al., 2018; Babajani et al.,  
319 2019a; Feigl et al., 2019; Malheiros et al., 2019).  
320 Moreover, nSe, in a dose-dependent manner, affected the activities of nitrate reductase enzyme  
321 (a key enzyme involved in the reduction of nitrate to nitrite), activities of two main antioxidant  
322 enzymes (catalase and peroxidase), and accumulation of proline (a vital amino acid with  
323 multifunctional protective roles). At low doses, the nSe-mediated induction in the nitrate  
324 reductase activity (an appropriate indicator in primary metabolism) may be considered an  
325 underlying mechanism responsible for subsequent stimulation of growth indices. However, its  
326 high concentrations may induce toxicity through the disruption of nitrogen assimilation  
327 processes. In line with our findings, the exposure to nSe has been reported to modulate  
328 accumulation of proline (Nazerieh et al., 2018), activity of nitrate reductase (Nazerieh et al.,  
329 2018; Safari et al., 2018; Babajani et al., 2019a), and the antioxidant system (Quiterio-Gutiérrez  
330 et al., 2019). There is a close interplay between the nitrate reductase activity and nitric oxide  
331 level in Se-treated plants (Lehotai et al., 2012; Nazerieh et al., 2018; Babajani et al., 2019a). In  
332 strawberry, for instance, the foliar-applied nSe enhanced the production of the hormone auxin,  
333 thereby improving root biomass and enhancing water and nutrient uptake (Zahedi et al., 2019).  
334 Moreover, nSe treatments stimulated secondary metabolism as indicated by induction of PAL  
335 activity and an increase in soluble phenols. In agreement with our findings, nSe was reported to  
336 be associated with stimulation of secondary metabolism through upregulations in the expression  
337 of RAS and HPPR genes in *Melissa officinalis* (Babajani et al., 2019a).

## 338 5. Conclusion

339 Herein, the supplementation of the culture medium with nSe is introduced as a promising  
340 approach to modify growth, morphology, metabolism, and anatomy. These findings provide

341 novel insights into the advantage/phytotoxicity of using nSe as a supplement in the culture  
 342 medium. Based on the MSAP analysis, nSe made substantial epigenetic variation in DNA  
 343 cytosine methylation. The nSe toxicity was associated with DNA hyper-methylations. Our  
 344 experiments provide the physiological, anatomical, and molecular bases to set optimized doses  
 345 for possible functions in plant cell and tissue cultures, clarify the involved mechanisms, and  
 346 scientifically exhibit the eco-toxicological risks of nSe pollution. Moreover, this study highlights  
 347 the fundamental involvement of transcription factors in conferring the changed growth,  
 348 morphology, development, and metabolism in response to nSe. Furthermore, the findings of the  
 349 present study underline the necessity of including epigenetic monitoring (DNA methylation,  
 350 histone acetylation/methylation, and miRNA) in toxicological evaluation of nanomaterials and  
 351 their impacts on various biological systems.

### 352 **CRediT authorship contribution statement**

353 Soheila Sotoodehnia Korani: Resources, methodology, review, and editing; Alireza  
 354 Iranbakhsh: Conceptualization, visualization, investigation, formal analysis, writing- original  
 355 draft, review, and editing; Mostafa Ebadi: Conceptualization, visualization, investigation,  
 356 software analysis, review, and editing; Ahmad Majd: Conceptualization, Investigation, review,  
 357 and editing. Zahra Oraghi Ardebili: Conceptualization, visualization, investigation, formal  
 358 analysis, writing, review, and editing.

### 359 **Declaration of competing interest**

360 The authors declare that they have no conflict of interest.

### 361 **Acknowledgments**

362 The authors would like to thank Prof. Emad Tajkhorshid, Dr. Narges Oraghi Ardebili and Dr.  
 363 Sara Rajaee-Behbahani for their benevolent and professional collaborations in the research  
 364 procedure.

365 **References**

- 366 Babajani, A., Iranbakhsh, A., Ardebili, Z.O. and Eslami, B., 2019a. differential growth, nutrition,  
 367 physiology, and gene expression in *Melissa officinalis* mediated by zinc oxide and elemental  
 368 selenium nanoparticles. *Environ. Sci. Pollut. Res.* 26, 24430–24444  
 369 <https://doi.org/10.1007/s11356-019-05676-z>
- 370 Babajani, A., Iranbakhsh, A., Ardebili, Z.O. and Eslami, B., 2019b. seed priming with non-  
 371 thermal plasma modified plant reactions to selenium or zinc oxide nanoparticles: cold plasma as  
 372 a novel emerging tool for plant science. *Plasma Chem. Plasma Process.* 39, 21–34.  
 373 <https://doi.org/10.1007/s11090-018-9934-y>
- 374 Bakshi, M. and Oelmüller, R., 2014. WRKY transcription factors: Jack of many trades in  
 375 plants. *Plant Signal. Behav.* 9, p.e27700.
- 376 Bates, L., Waldren, R., and Teare, I. 1973. rapid determination of free proline for water-stress  
 377 studies. *Plant Soil* 39, 205-207. doi:10.1007/BF00018060
- 378 Beaudoin-Eagan, L., D., Thorpe, T., A., 1985. tyrosine and phenylalanine ammonia lyase  
 379 activities during shoot initiation in tobacco callus cultures. *Plant Physiol.* 78,438–441
- 380 Brzóska, K., Grądzka, I. and Kruszewski, M., 2019. silver, gold, and iron oxide nanoparticles  
 381 Alter miRNA expression but do not affect DNA methylation in HepG2 cells. *Materials* 12,  
 382 p.1038. hanisms of Mutagenesis, 774, 49-58.

- 383 Cao, D., Liu, Y., Ma, L., Jin, X., Guo, G., Tan, R., Liu, Z., Zheng, L., Ye, F. and Liu, W., 2018.  
 384 transcriptome analysis of differentially expressed genes involved in selenium accumulation in tea  
 385 plant (*Camellia sinensis*). PloS One 13, p.e0197506.
- 386 Djanaguiraman, M., Belliraj, N., Bossmann, S., Prasad, P.V., 2018. high temperature stress  
 387 alleviation by selenium nanoparticle treatment in grain sorghum. ACS Omega 3, 2479–2491  
 388 Feigl, G., Horváth, E., Molnár, Á., Oláh, D., Poór, P. and Kolbert, Z., 2019. ethylene-nitric oxide  
 389 interplay during selenium-induced lateral root emergence in *Arabidopsis*. J. Plant Growth Regul.  
 390 38, 1481–1488.
- 391 Ghasempour, M., Iranbakhsh, A., Ebadi, M., Ardebili, Z.O., 2019. multi-walled carbon  
 392 nanotubes improved growth, anatomy, physiology, secondary metabolism, and callus  
 393 performance in *Catharanthus roseus*: an in vitro study. 3 Biotech, 9, 404.  
 394 <https://doi.org/10.1007/s13205-019-1934-y>
- 395 Ghosh, M., Bhadra, S., Adegoke, A., Bandyopadhyay, M. and Mukherjee, A., 2015. MWCNT  
 396 uptake in *Allium cepa* root cells induces cytotoxic and genotoxic responses and results in DNA  
 397 hyper-methylation. Mutat. Res. 774, 49-58
- 398 Guevara, M.Á., de María, N., Sáez-Laguna, E., Vélez, M.D., Cervera, M.T. and Cabezas, J.A.,  
 399 2017. analysis of DNA cytosine methylation patterns using methylation-sensitive amplification  
 400 polymorphism (MSAP). In Plant Epigenetics (99-112). Humana Press, Boston, MA.  
 401 DOI:10.1007/978-1-4899-7708-3\_9
- 402 Hu, T., Li, H., Li, J., Zhao, G., Wu, W., Liu, L., Wang, Q., Guo, Y., 2018. absorption and bio-  
 403 transformation of selenium nanoparticles by wheat seedlings (*Triticum aestivum* L). Front. Plant  
 404 Sci. 9, 597

- 405 Iranbakhsh, A., Ardebili, Z.O., Ardebili, N.O., Ghoranneviss, M., Safari, N., 2018. cold plasma  
 406 relieved toxicity signs of nano zinc oxide in *Capsicum annuum* cayenne via modifying growth,  
 407 differentiation, and physiology. *Acta Physiol. Plant.* 40, 154.
- 408 Iranbakhsh, A., Oraghi Ardebili, Z., Molaei, H., Oraghi Ardebili, N., Amini, M., 2020. cold  
 409 plasma up-regulated Expressions of WRKY1 transcription factor and genes involved in  
 410 biosynthesis of cannabinoids in hemp (*Cannabis sativa* L.). *Plasma Chem. Plasma*  
 411 *Process.* 40, 527–537. <https://doi.org/10.1007/s11090-020-10058-2>
- 412 Khan, S.A., Li, M.Z., Wang, S.M. and Yin, H.J., 2018. revisiting the role of plant transcription  
 413 factors in the battle against abiotic stress. *Int. J. Mol. Sci.* 19, 1634.
- 414 Kolbert, Z., Molnár, Á., Feigl, G. and van Hoewyk, D., 2018. plant selenium toxicity: Proteome  
 415 in the crosshairs. *J. Plant Physiol.* 232, 291-300. <https://doi.org/10.1016/j.jplph.2018.11.003>
- 416 Kumar, G., Bajpai, R., Sarkar, A., Mishra, R.K., Gupta, V.K., Singh, H.B. and Sarma, B.K.,  
 417 2019. identification, characterization and expression profiles of *Fusarium udum* stress-responsive  
 418 WRKY transcription factors in *Cajanus cajan* under the influence of NaCl stress and  
 419 *Pseudomonas fluorescens* OKC. *Sci. Rep.* 9, 1-9.
- 420 Lehota, N., Kolbert, Z., Pető, A., Feigl, G., Ördög, A., Kumar, D., Tari, I., Erdei, L., 2012.  
 421 selenite-induced hormonal and signalling mechanisms during root growth of *Arabidopsis*  
 422 *thaliana* L. *J. Exp. Bot.* 63, 5677-5687.
- 423 Lehota, N., Feigl, G., Koós, Á., Molnár, Á., Ördög, A., Pető, A., Erdei, L. and Kolbert, Z., 2016.  
 424 nitric oxide–cytokinin interplay influences selenite sensitivity in *Arabidopsis*. *Plant Cell Rep.* 35,  
 425 2181-2195.

- 426 Malheiros, R.S., Costa, L.C., Ávila, R.T., Pimenta, T.M., Teixeira, L.S., Brito, F.A., Zsögön, A.,  
 427 Araújo, W.L. and Ribeiro, D.M., 2019. selenium downregulates auxin and ethylene biosynthesis  
 428 in rice seedlings to modify primary metabolism and root architecture. *Planta* 250, 333–345.  
 429 <https://doi.org/10.1007/s00425-019-03175-6>
- 430 Marchive, C., Léon, C., Kappel, C., Coutos-Thévenot, P., Corio-Costet, M.F., Delrot, S. and  
 431 Lauvergeat, V., 2013. Over-expression of VvWRKY1 in grapevines induces expression of  
 432 jasmonic acid pathway-related genes and confers higher tolerance to the downy mildew. *PLoS*  
 433 One 8, p.e54185.
- 434 Moghanloo, M, Iranbakhsh, A, Ebadi, M, Ardebili, ZO 2019a. Differential physiology and  
 435 expression of phenylalanine ammonia lyase (PAL) and universal stress protein (USP) in the  
 436 endangered species *Astragalus fridae* following seed priming with cold plasma and manipulation  
 437 of culture medium with silica nanoparticles. *3Biotech* 9, 288
- 438 Moghanloo, M, Iranbakhsh, A, Ebadi, M, Satari, TN, Ardebili, ZO, 2019b. seed priming with  
 439 cold plasma and supplementation of culture medium with silicon nanoparticle modified growth,  
 440 physiology, and anatomy in *Astragalus fridae* as an endangered species. *Acta Physiol. Plant.* 41,  
 441 54
- 442 Murashige, T., Skoog, F., 1962. a revised medium for rapid growth and bio assays with tobacco  
 443 tissue cultures. *Physiol. Plant* 15, 473–497
- 444 Nazerieh, H., Ardebili, Z.O., Iranbakhsh, A., 2018. potential benefits and toxicity of  
 445 nanoselenium and nitric oxide in peppermint. *Acta Agric. Slov.* 111, 357-368.
- 446 Quiterio-Gutiérrez, T., Ortega-Ortiz, H., Cadenas-Pliego, G., Hernández-Fuentes, A.D.,  
 447 Sandoval-Rangel, A., Benavides-Mendoza, A., Cabrera-de la Fuente, M. and Juárez-Maldonado,

- 448 A., 2019. the application of selenium and copper nanoparticles modifies the biochemical  
 449 responses of tomato Plants under stress by *Alternaria solani*. Int. J. Mol. Sci. 20, p.1950.
- 450 Safari, M., Ardebili, Z.O. and Iranbakhsh, A., 2018. selenium nano-particle induced alterations  
 451 in expression patterns of heat shock factor A4A (HSFA4A), and high molecular weight glutenin  
 452 subunit 1Bx (Glu-1Bx) and enhanced nitrate reductase activity in wheat (*Triticum aestivum*  
 453 L.). Acta Physiol. Plant. 40, p.117.
- 454 Safari, N., Iranbakhsh, A. and Ardebili, Z.O., 2017. non-thermal plasma modified growth and  
 455 differentiation process of Capsicum annuum PP805 Godiva in in vitro conditions. Plasma Sci.  
 456 Technol. 19, p.055501.
- 457 Salah, S.M., Yajing, G., Dongdong, C., Jie, L., Aamir, N., Qijuan, H., Weimin, H., Mingyu, N.  
 458 and Jin, H., 2015. Seed priming with polyethylene glycol regulating the physiological and  
 459 molecular mechanism in rice (*Oryza sativa* L.) under nano-ZnO stress. Sci. Rep. 5, p.14278.
- 460 Seddighinia, F.S., Iranbakhsh, A., Ardebili, Z.O., Satari, T.N. and Soleimanpour, S., 2020. seed  
 461 priming with cold plasma and multi-walled carbon nanotubes modified growth, tissue  
 462 differentiation, anatomy, and yield in bitter melon (*Momordica charantia*). J. Plant Growth  
 463 Regul. 39, 87–98. <https://doi.org/10.1007/s00344-019-09965-2>
- 464 Sharma, P.D., Singh, N., Ahuja, P.S. and Reddy, T.V., 2011. abscisic acid response element  
 465 binding factor 1 is required for establishment of Arabidopsis seedlings during winter. Molecular  
 466 Biology Reports 38, 5147-5159.
- 467 Soleymanzadeh, R., Iranbakhsh, A., Habibi, G. and Oraghi Ardebili, Z., 2020. selenium  
 468 nanoparticle protected strawberry against salt stress through modifications in salicylic acid, ion  
 469 homeostasis, antioxidant machinery, and photosynthesis performance. Acta Biol. Cracovien. Ser.  
 470 Bot. DOI: 10.24425/abcsb.2019.127751

471 Song, H., Sun, W., Yang, G. and Sun, J., 2018. WRKY transcription factors in legumes. BMC  
472 Plant Biol. 18, p.243.

473 Sym, G.J. 1984. optimisation of the in vivo assay conditions for nitrate reductase in barley  
474 (*Hordeum vulgare* L. cv. Igri). J. Sci. Food Agric. 35, 725-30. doi:10.1002/jsfa.2740350703

475 Zahedi, S.M., Abdelrahman, M., Hosseini, M.S., Hoveizeh, N.F. and Tran, L.S.P., 2019.  
476 alleviation of the effect of salinity on growth and yield of strawberry by foliar spray of selenium-  
477 nanoparticles. Environ. Pollut. <https://doi.org/10.1016/j.envpol.2019.04.078>

478

479

480

481

482

483

484

485

486

487

488

489

490

491 **Figure captions:**

492 **Fig. 1-** The nSe physicochemical traits, including UV-Vis scan spectrum curves at 10 (a) and 20  
 493 (b)  $\text{mgL}^{-1}$  (A), the zeta potential spectrum (B), and transmission electron microscopy (TEM)  
 494 image (C).

495 **Fig. 2-** variations in morphology and growth of seedlings grown in culture medium containing  
 496 different doses of BSe/nSe. A- Control; B- BSe of  $0.5 \text{ mgL}^{-1}$ ; C- nSe of  $0.5 \text{ mgL}^{-1}$ ; D- BSe of  $1 \text{ mgL}^{-1}$ ;  
 497 E- nSe of  $1 \text{ mgL}^{-1}$ ; F- BSe of  $10 \text{ mgL}^{-1}$ ; G- nSe of  $10 \text{ mgL}^{-1}$ ; H- BSe of  $30 \text{ mgL}^{-1}$ ; I- nSe  
 498 of  $30 \text{ mgL}^{-1}$ ; J- total fresh mass of leaves; K- root fresh mass; Descriptions of treatment groups  
 499 in J and K sections: C- Control; BSe0.5- BSe at  $0.5 \text{ mgL}^{-1}$ ; nSe0.5- nSe at  $0.5 \text{ mgL}^{-1}$ ; BSe1- BSe  
 500 at  $1 \text{ mgL}^{-1}$ ; nSe1- nSe at  $1 \text{ mgL}^{-1}$ ; BSe10- BSe at  $10 \text{ mgL}^{-1}$ ; nSe10- nSe at  $10 \text{ mgL}^{-1}$ ; BSe30- BSe  
 501 at  $30 \text{ mgL}^{-1}$ ; nSe30- nSe at  $30 \text{ mgL}^{-1}$ ; Significance levels: \*:  $0.05 \leq P \leq 0.01$ ; \*\*:  $0.01 < P \leq 0.005$ ;  
 502 \*\*\*:  $0.005 < P \leq 0.001$ ; \*\*\*\*:  $P < 0.001$

503 **Fig. 3-** MSAP-based variation in DNA methylation patterns of pepper in response to the  
 504 incorporation of nSe at 0 (control) and  $10 \text{ mgL}^{-1}$  into the MS culture medium; A-Principal  
 505 coordinates analysis (PCoA) plots of variation in DNA methylation under *Eco RI/Hpa* II  
 506 conditions; B- Clustering dendrogram based on DNA methylation variation between control (C),  
 507 and nSe treatment groups; C- Percentage of molecular variance within/among treatment groups.

508 **Fig. 4-** MSAP-based variation in DNA methylation patterns of pepper in response to the  
 509 incorporation of nSe at 0 (control) and  $10 \text{ mgL}^{-1}$  into the MS culture medium; A-Principal  
 510 coordinates analysis (PCoA) plots of variation in DNA methylation under *Eco RI/Msp* I  
 511 conditions; B- Clustering dendrogram based on DNA methylation variation between control (C),

512 and nSe treatment groups; C- Percentage of molecular variance within and among treatment  
 513 groups.

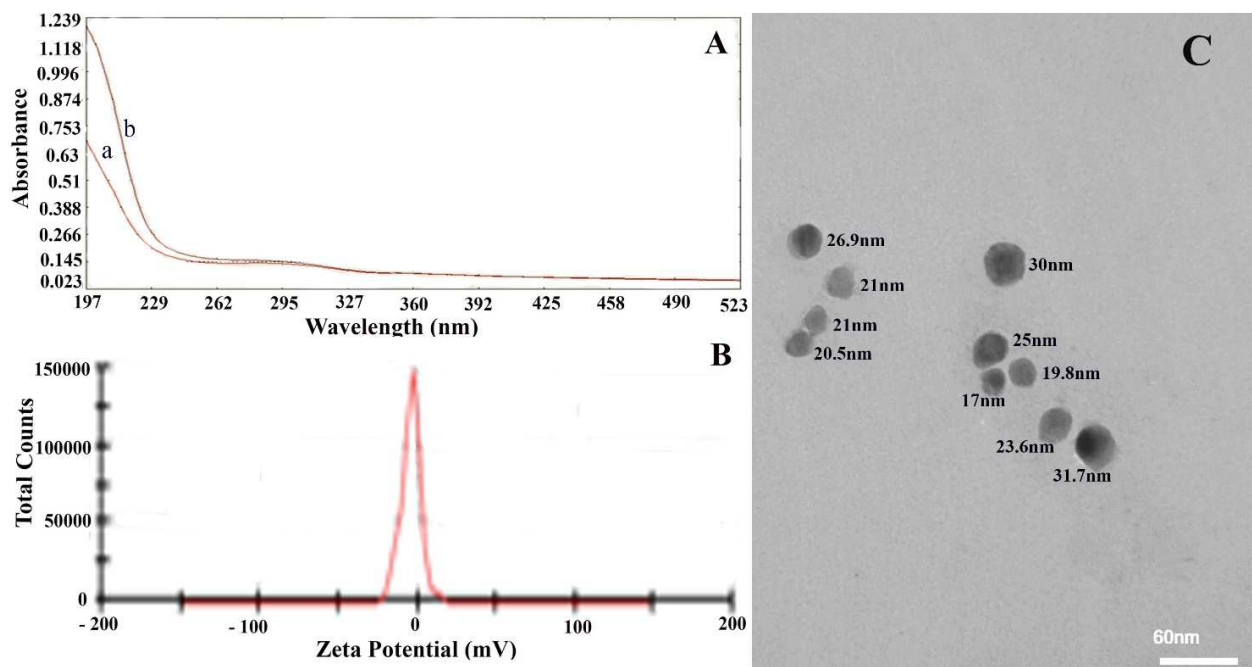
514 **Fig. 5-** MSAP-based variation in DNA methylation patterns of pepper in response to the  
 515 incorporation of nSe at 0 (control) and  $10 \text{ mgL}^{-1}$  into the MS culture medium. A- A  
 516 representative gel image exhibiting polymorphic fragments in control and nSe-counteracted  
 517 seedlings. B- Principal coordinates analysis (PCoA) plot of variation in DNA methylation under  
 518 both *Eco RI/Msp I* and *Eco RI/Msp I* conditions; C- PCoA plot exhibiting the nSe-associated  
 519 epigenetic variation (MSL) in DNA cytosine methylation; Long axis in ellipse shapes indicates  
 520 the direction of maximum dispersion, while the short axis shows the minimum dispersion  
 521 direction.

522 **Fig. 6-** The nSe-associated changes in expression of the bZIP1 (A) and WRKY1 (B)  
 523 transcription factors as well as variations in physiological traits, including nitrate reductase  
 524 activity (C), proline concentration (D), peroxidase activity (E), catalase activity (F), PAL activity  
 525 (G), and concentrations of total soluble phenols (H). Descriptions of treatment groups: C-  
 526 Control; nSe0.5- nSe of  $0.5 \text{ mgL}^{-1}$ ; nSe1- nSe of  $1 \text{ mgL}^{-1}$ ; nSe10- nSe of  $10 \text{ mgL}^{-1}$ ; Significance  
 527 levels: \*:  $0.05 \leq P \leq 0.01$ ; \*\*:  $0.01 < P \leq 0.005$ ; \*\*\*:  $0.005 < P \leq 0.001$ ; \*\*\*\*:  $P < 0.001$

528 **Fig. 7-** The differential morphology and structure of stem apical meristem (SAM) in response to  
 529 supplementation of MS medium with different doses of nSe, including 0 (A), 1 (B), and  $10 \text{ mgL}^{-1}$   
 530 (C). Microscopic images were taken at a 10X magnification.

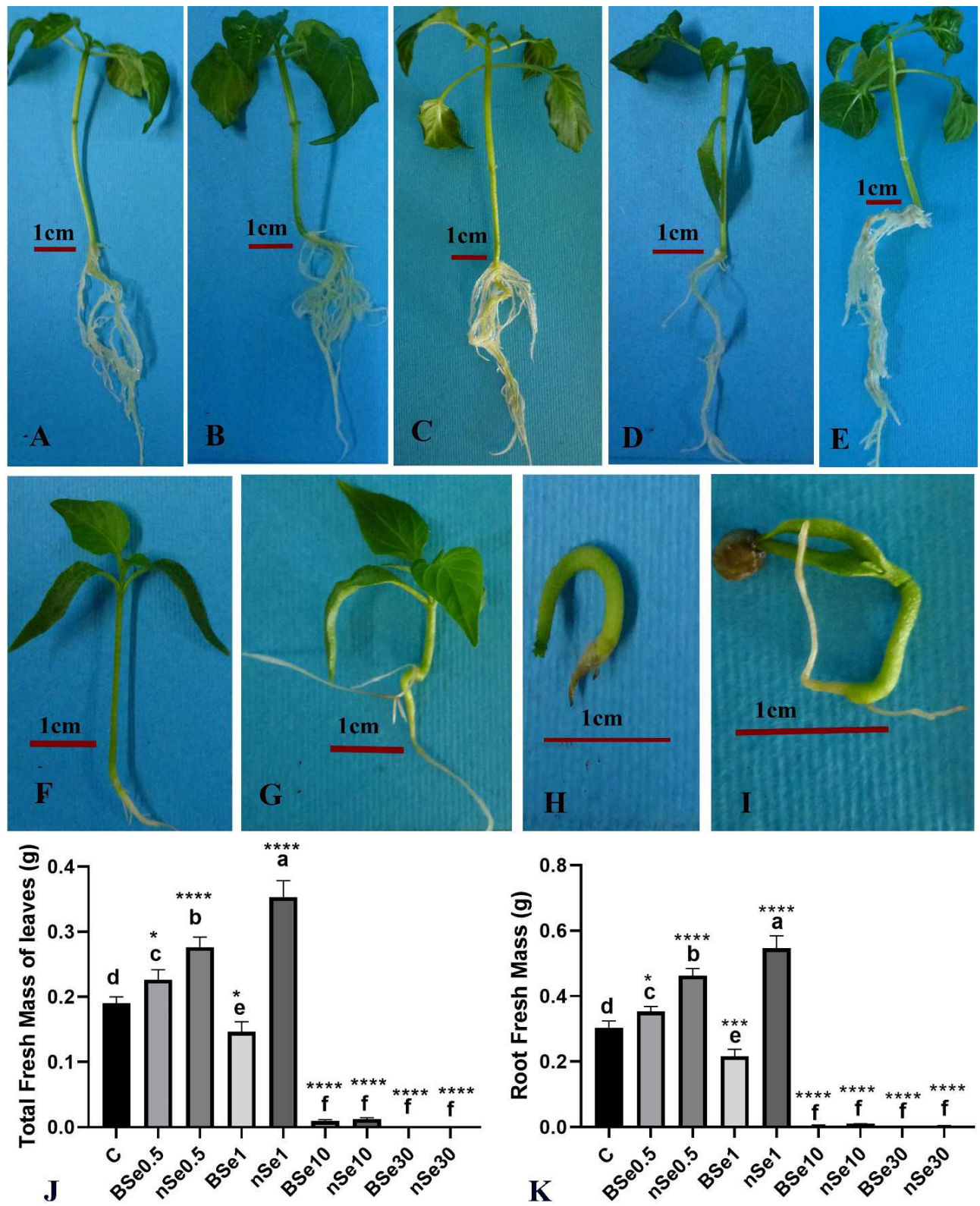
531 **Fig. 8-** The cross-sections of basal stems (A-D) and root (E-J) of 35-day old pepper seedlings  
 532 cultured in the hormone-free MS medium containing different doses of nSe. A- Control; B- nSe  
 533 of  $1 \text{ mgL}^{-1}$ ; C- nSe of  $10 \text{ mgL}^{-1}$ ; D- nSe of  $30 \text{ mgL}^{-1}$ . E- Control; F- nSe of  $0.5 \text{ mgL}^{-1}$ ; G- nSe of  
 534  $1 \text{ mgL}^{-1}$ ; H- nSe of  $10 \text{ mgL}^{-1}$ . I1- nSe of  $30 \text{ mgL}^{-1}$ ; I2- enlarged view of the root central cylinder

535 of I1 section; a lack of differentiation of the vascular conducting tissues (xylem and phloem) in  
 536 root cylinder is indicated by an arrow. Pa- Parenchyma, Xy- Xylem; Microscopic images were  
 537 taken at a 10X magnification.



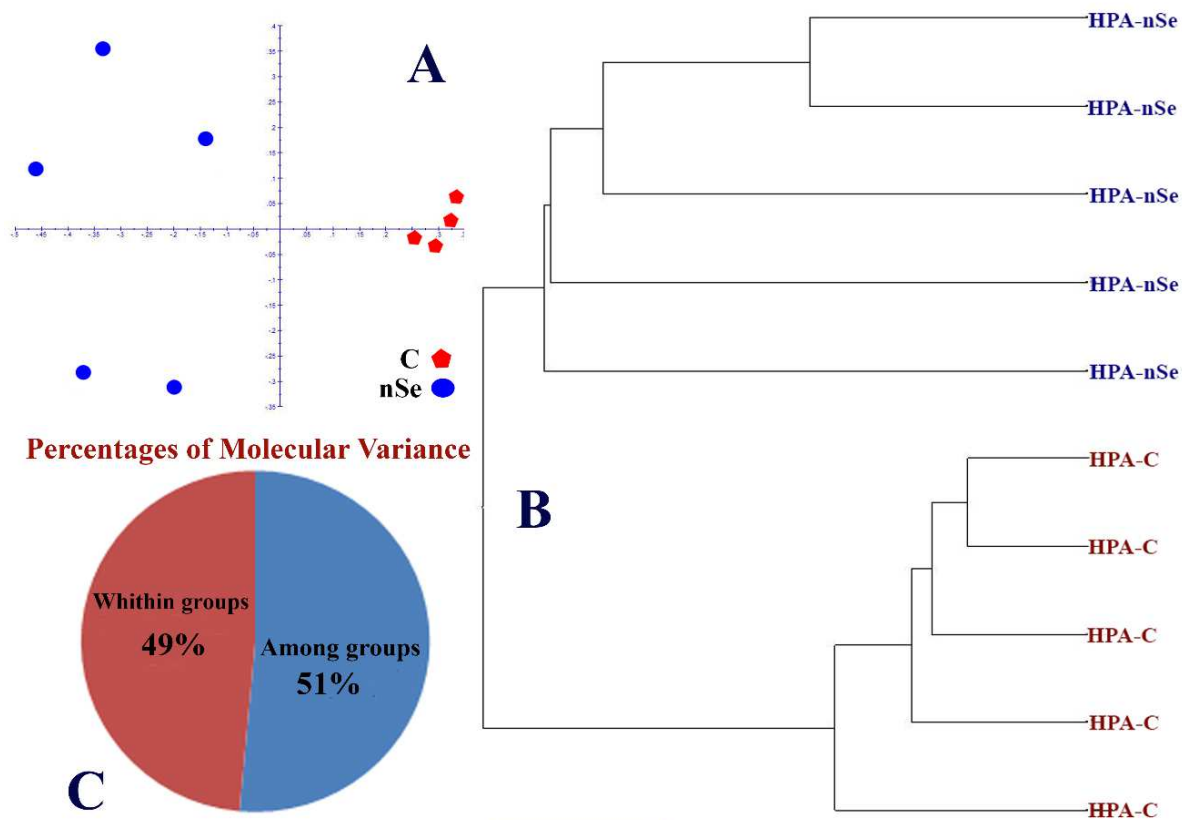
538

539 **Fig. 1**



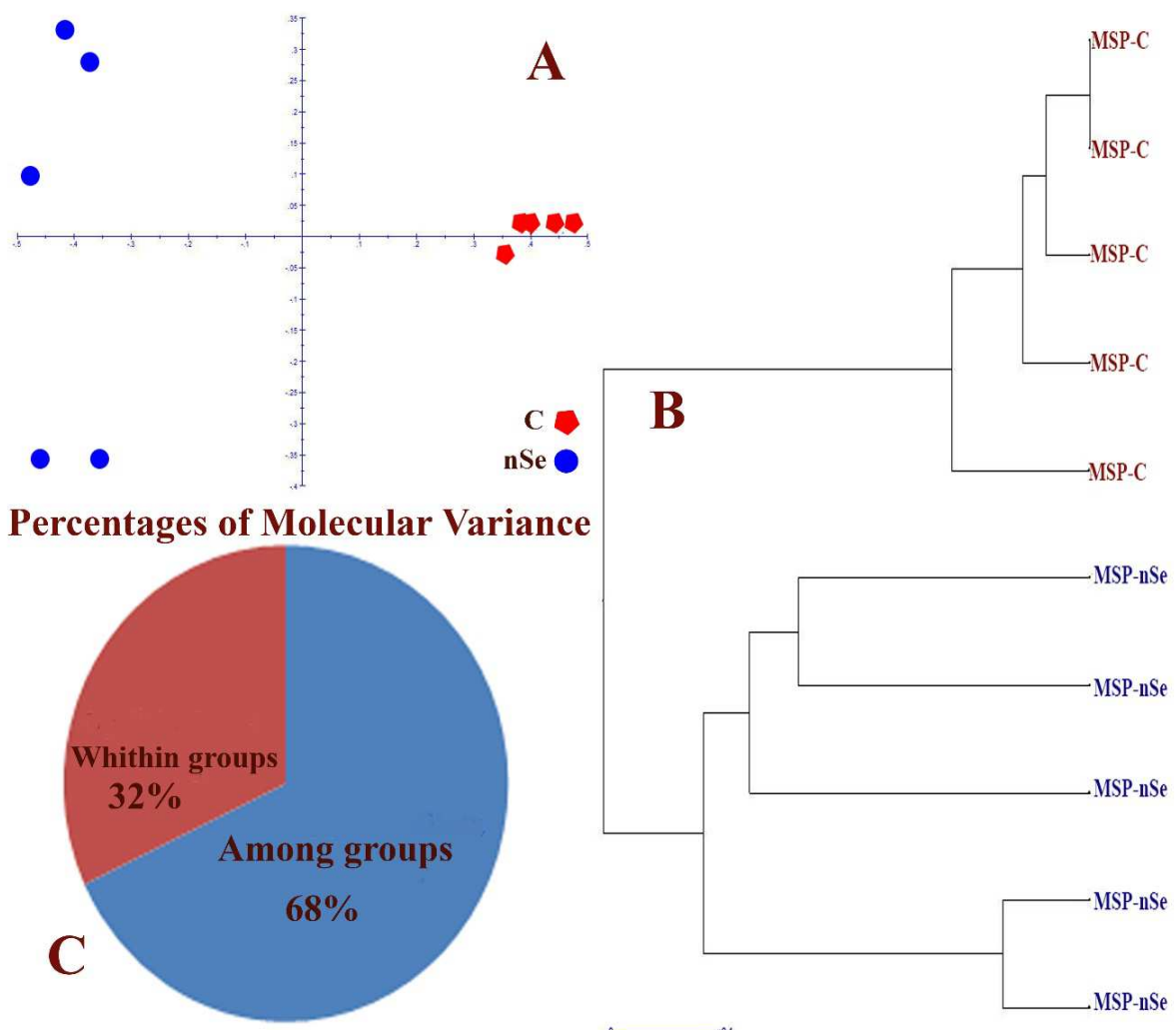
540

541 Fig. 2



542

543 **Fig. 3**



544

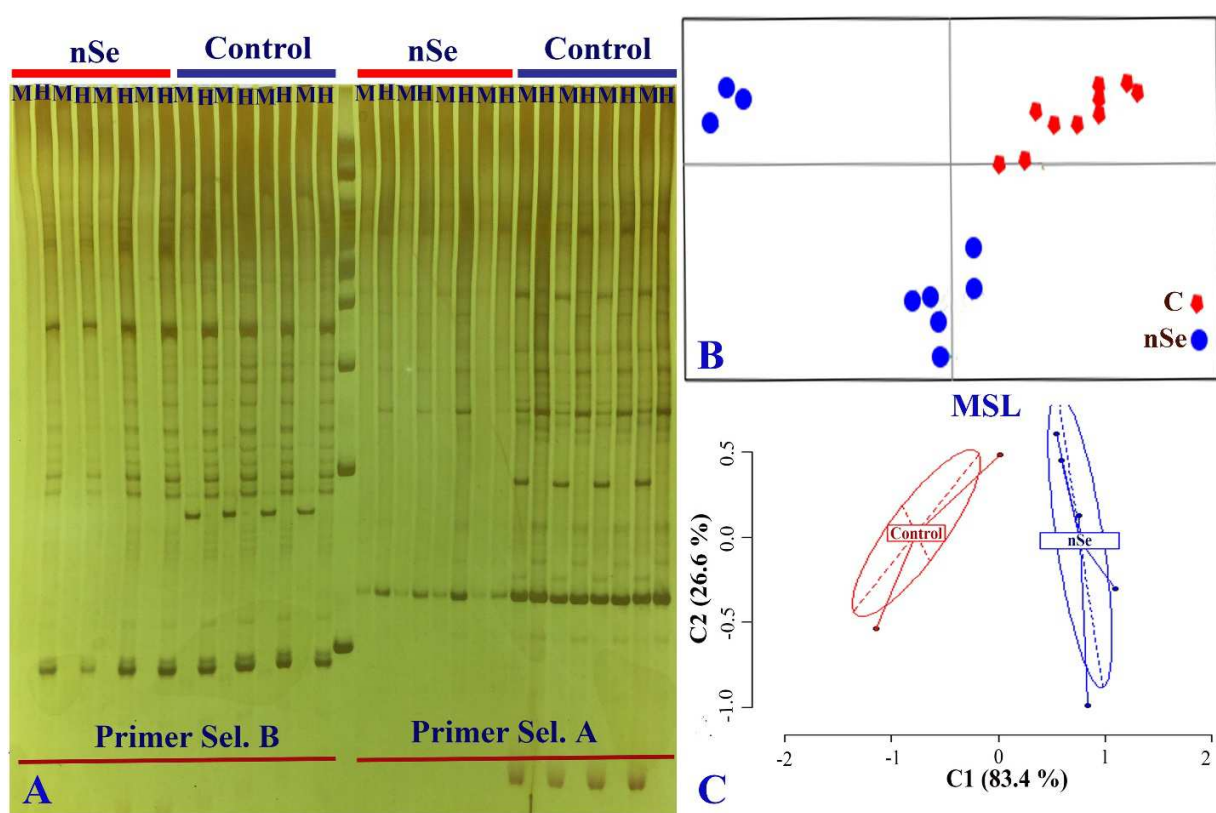
545 **Fig. 4**

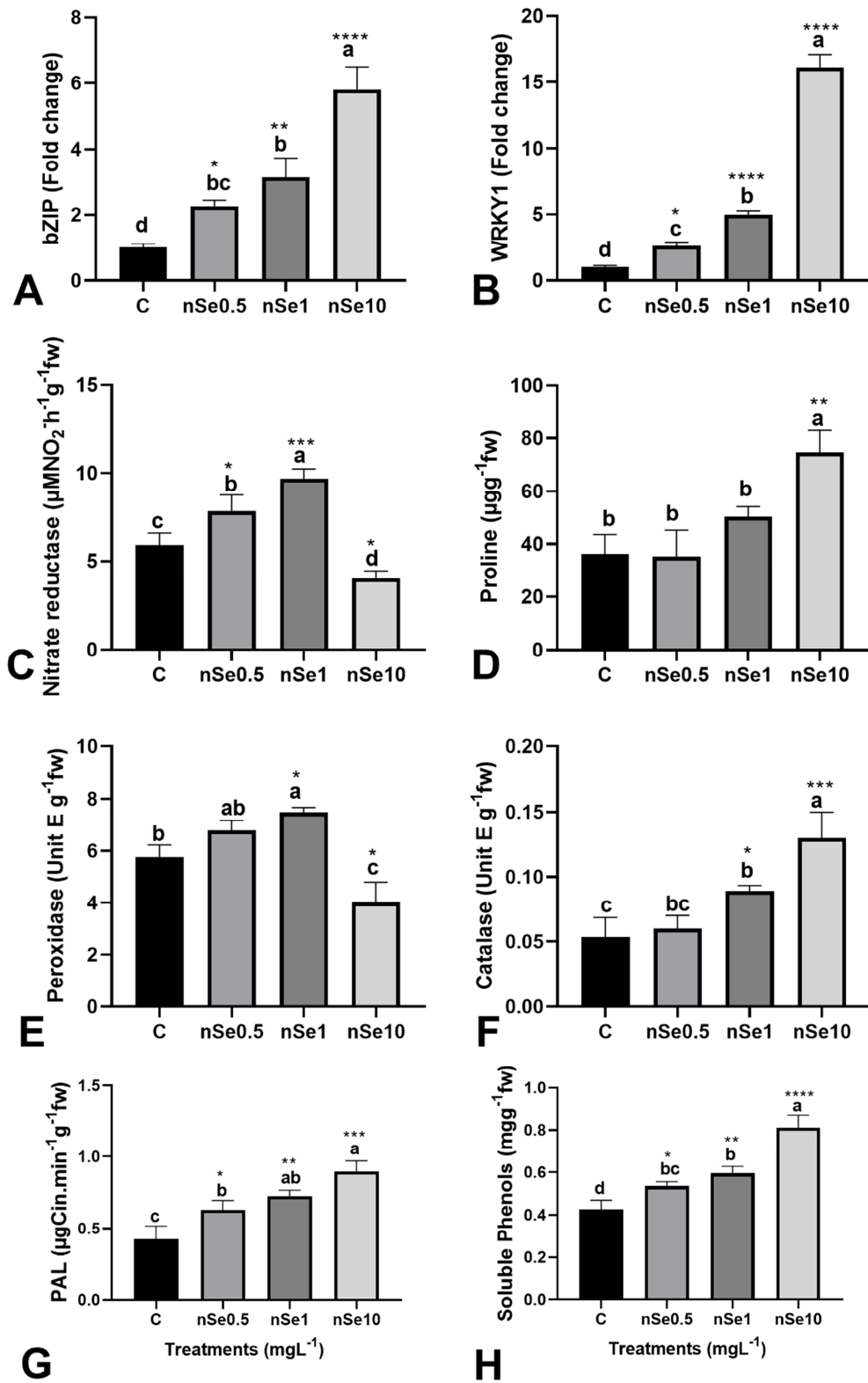
546

547 **Fig. 5**

548

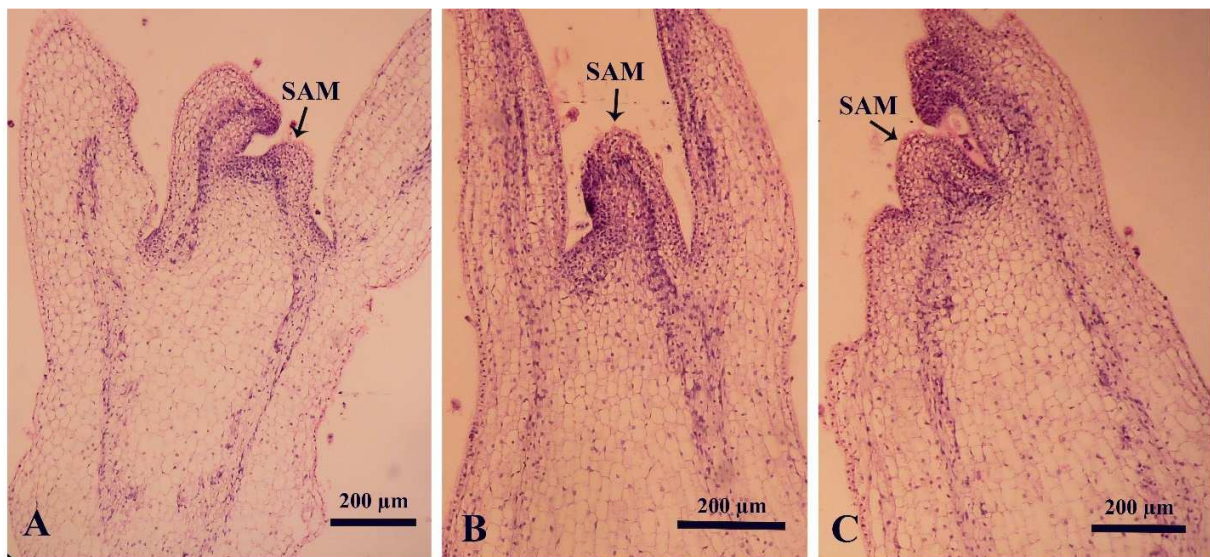
549





550

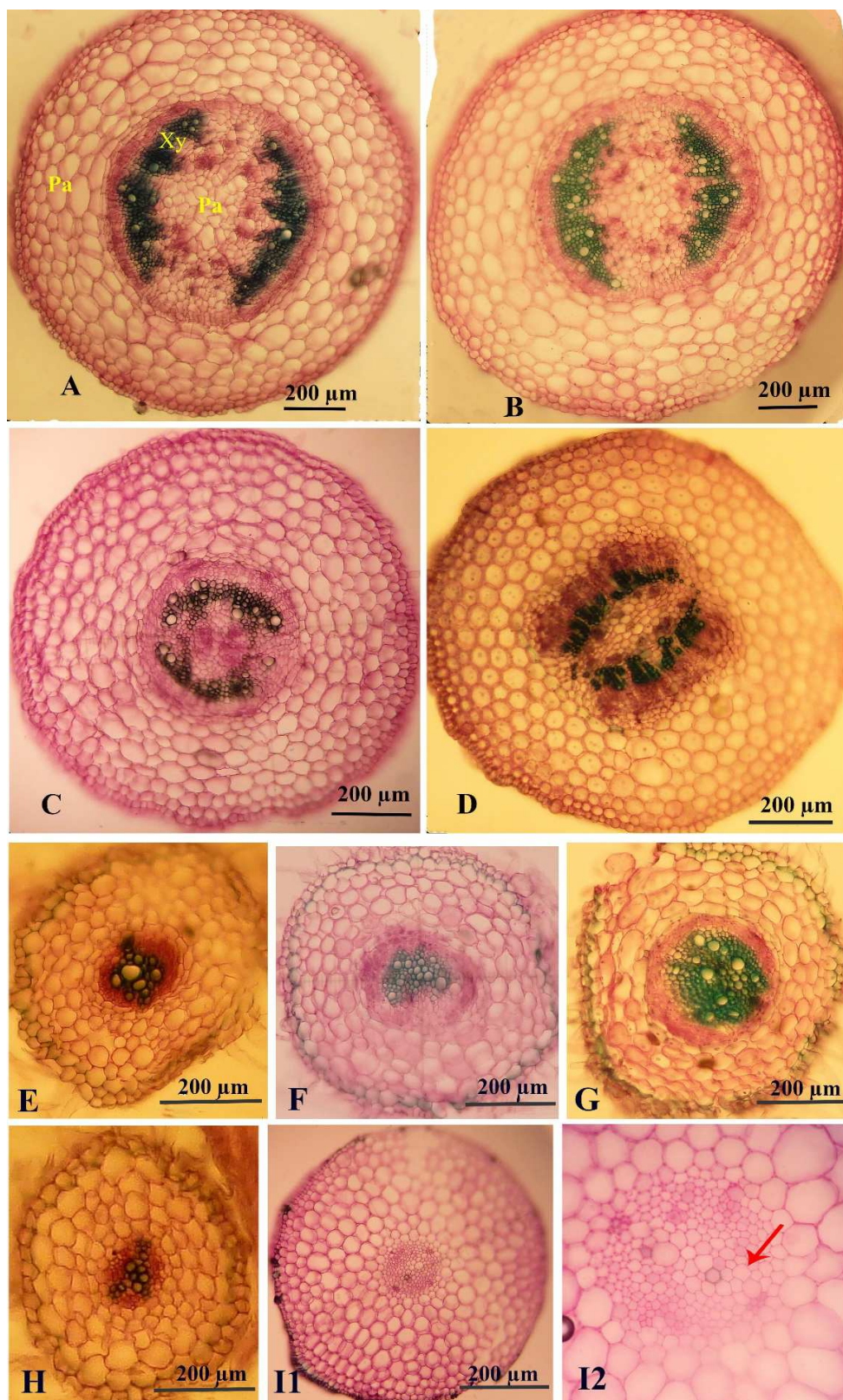
551 Fig. 6



552  
553

**Fig. 7**

554



555

556 **Fig. 8**

## Highlights

- Potential benefits/phytotoxicity of selenium nanoparticle (nSe) as a supplement
- Providing evidence on nSe-associated epigenetic changes
- nSe transcriptionally up-regulated bZIP1 and WRKY1 transcription factors
- nSe influenced growth, anatomy, and metabolism
- The nSe toxicity was associated with DNA hyper-methylations.

**Declaration of interests**

The authors declare that they have no known competing financial interests or personal relationships that could have appeared to influence the work reported in this paper.